ACS OMEGA

Open Access

http://pubs.acs.org/journal/acsodf

Article

Theoretical Modeling of $Sr(^{q+})$ He (q = 0, 1, 2) van der Waals Systems Including Spin−Orbit Coupling

Mohamed Bejaoui, Wissem Zrafi, Jamila Dhiflaoui,* and Hamid Berriche*

Cite This: *ACS Omega* 2024, 9, 32604−32616

Read Online

ACCESS | Metrics & More | Article Recommendations

ABSTRACT: Using an ab initio methodology that incorporates pseudopotential technique in conjunction with pair potential approaches, core polarization potentials (CPP), large basis sets of Gaussian type, and full configuration interaction calculations, we investigate interaction of neutral and charged Sr^{q+}(q = 0,1,2) with helium atom. In this context, the core−core interaction of Sr^{2+}-He is included using an accurately performed potential for the ground state at CCSD(T) level of calculation. Also, the potential energy curves and permanent and transition dipole moments of the ground state and numerous excited states have been performed respectively for Sr^{+}He and SrHe systems. Subsequently, the spin−orbit effect is considered by utilizing a semiempirical method for states dissociating into Sr^{+}(5p) + He, Sr^{+}(6p) + He, Sr^{+}(4d) + He, Sr^{+}(5d) + He, Sr(5s5p) + He, and Sr(5s4d) + He. The spectroscopic constants of the Sr^{q+}(q = 0, 1, 2) He states, with and without spin−orbit interaction, are derived and assessed in comparison to the existing theoretical and experimental studies. Such comparison has revealed good agreement, especially, for the Sr^{+}He ionic system. Additionally, the spin−orbit effect is considered for the $X^2\Sigma^+ \rightarrow 2^2\Pi_{1/2,3/2}$ and $X^2\Sigma^+ \rightarrow 3^2\Sigma_{1/2}{}^+$ transition dipole moments for Sr^{+}He.

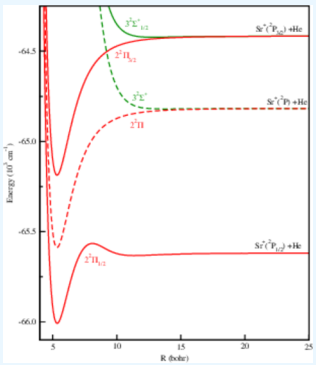

1. INTRODUCTION

Interactions between alkali and alkaline-earth elements with rare gas atoms are of significant importance in various realms of physics and chemistry. These interactions have been investigated theoretically and experimentally for many years and across numerous systems. However, there are aspects of several reasonably simple systems that remain not well understood. To gain a comprehensive understanding of these subtle interactions, it is essential to assess both theoretical approaches and basis sets.

The potential between pairs of entities can be utilized by theoreticians to simulate systems using molecular dynamics, providing a valuable resource for spectroscopists to enhance their comprehension and analysis of molecular spectra. Furthermore, interactions between alkali or alkaline-earth elements in their ground state and helium atoms may be even more subtle than those observed among helium atoms themselves. Alkaline-earth metals exhibit stronger binding to helium compared to their alkali metal counterparts; however, the metal−helium interaction is weaker than the self-interaction within helium.

Much less is known about the interaction between strontium and rare-gas atoms. Several experiments have been conducted to investigate phenomena such as line broadening, resonance line shifts, and alterations in the distribution of light resulting from collisions between strontium and rare-gas atoms, as documented in refs 1−6. To provide accurate and meaningful interpretations of these experiments, it is imperative to establish dependable potentials for both Sr^{+}-RG and Sr-RG interactions.

On the theoretical side, there have been several calculations of interactions between heavier alkaline-earth atoms and helium, as documented in refs 7−15. Stienkemeier et al.[7] observed absorption bands of alkaline-earth calcium and strontium atoms produced in superfluid helium droplets (He_n) at 0.4 K, where the excitation of the lowest singlet transitions shows large, blue-shifted peaks compared to atomic lines. Massimo and Fausto[8] studied the stability, structure, and experimental relevance of M^{+} (^{2}P) ^4He_n (M = Sr or Ba).

Gardner et al.[9] have provided ab initio potential energy curves for M^{q+}RG complexes, where q = 1 and 2; RG = He−Rn; and M = Ca, Sr, and Ba. On the other hand, Giusti-Suzor and Roueff[10,11] explored Ca^{+} and Sr^{+} perturbed by He using a semiclassical method. They introduced a modeled potential known as the exchange interaction, incorporating a Fermi-type repulsive interaction between the valence electron and the RG atom. Harima et al.[12] determined the potential energy for alkaline earth ion (Sr^{+}, Ca^{+}, and Mg^{+}) and RG atom (Ar, He) pairs using the pseudopotential model of Baylis.[13]

Received: February 14, 2024
Revised: June 20, 2024
Accepted: July 9, 2024
Published: July 15, 2024

Lovallo et al.[14] utilized the well-tempered model core potential method to investigate interactions between heavier Group 2 akaline-earth metals (Ca, Sr, and Ba) and helium rare gas. Their calculated pair potentials were determined at the coupled-cluster level of theory, and the corresponding pair-potential parameters were used to predict the solvation of Ca, Sr and Ba atoms by a helium nanodroplet. Unfortunately, results from these calculations differ considerably from each other. Among all strontium rare-gas complexes, SrAr is the only complex for which interaction potential is determined experimentally, in one supersonic beam experiment.[4] For the same system, SrAr, Zhu et al.[5] conducted an MCSCF calculation, with their results in reasonable agreement with the experimental ones. Yin et al.[15] used a model potential proposed by Tang and Toennis (TT)[16] to generate the ground state interaction potential for Sr-RG complexes, where RG = He, Ne, Ar, Kr, and Xe.

Recently, Kreis et al.[17,18] have reported measurements by high resolution photoionization, photoelectron, and photo-dissociation spectroscopy of the structure and dynamics of the lowest three electronic states of $MgKr^+$ and $MgNe^+$ systems.

To the best of our knowledge, this is the first theoretical study of the $SrHe^+$ and SrHe molecules to compute the first 12 and 13 low-lying excited states, respectively. Additionally, the permanent and transition dipole moments among specific states and the spin−orbit effects have been investigated. Our results offer unprecedented insights into the electronic structure and optical properties of these important molecules, which are of fundamental and technological interest to researchers in various fields, including cold molecular physics, molecular spectroscopy, and quantum chemistry.

In this work, we provide a detailed explanation of the computational methods used in Section 2. In Section 3, we present and discuss the results obtained for the $Sr^{q+}He$ (q = 0, 1, 2) ionic and neutral systems, both with and without spin−orbit coupling, for the ground state and several excited states. Finally, we draw our conclusions in Section 4.

2. COMPUTATIONAL METHODS

The potential energy curves of Sr^{q+}(q = 0, 1) interacting with the Helium atom are determined using the same model potential employed in several previous studies in our group,[19−25] primarily, for the alkali-RG dimers. Both helium and the Sr^{2+} ion is considered as whole cores and are substituted with effective potentials. The total potential (V_{tot}) is calculated by summing up three contributions

$$V_{tot} = V_{Sr^{2+}He} + V_{qe\text{-}Sr^{2+}He} + V_{SO} \quad (q = 1 \text{ or } 2)$$

The first, second, and third terms denote, respectively, the core−core interaction, the interaction between the valence electron(s) and the ionic system $Sr^{2+}He$ in its ground state, and finally, the spin−orbit interaction. These terms will be elaborated upon in the following section.

2.1. The Core−Core Interaction ($V_{Sr^{2+}He}$). The potential energy of Sr^{2+}-He, representing the core−core interaction in the model, is calculated separately at Restricted Coupled Cluster Single, Double and Triple excitation (CCSD (T)) level of theory, as implemented in the Molpro program.[26]

For this ionic molecular system, we are only interested in the ground state, as it will be utilized as the core−core potential in modeling Sr^+He and SrHe. The ground state potential energy is determined at the CCSD(T) level calculation using d-aug-cc-PV5Z basis set for the helium atom and the basis set referenced in ref 27,28 for the for strontium.

The accuracy of the $Sr^{2+}He$ ground state potential energy is crucial for investigating the Sr^+He, SrHe and, in the future, $Sr^{q+}He_n$ (q = 1, 2) clusters. Indeed, the precision of all electronic states of the $Sr^{q+}He$ (q = 0, 1) will depend on the accuracy of the $Sr^{2+}He$ ground state potential interaction. Calculations of the potential energy for the doubly charged molecular system have been performed over a wide and dense range of internuclear distances. Furthermore, two potential models, Tang and Toennies (TT)[16] and Extended Lennard-Jones (ELJ)[29] were employed to fit the potential energy curve of $Sr^{2+}He$. Given that this core−core interaction will be utilized in the Sr^+He and SrHe modeling, a comprehensive analytical description is necessary across all distance ranges.

In the TT model, the long-range attractive potential $\frac{-C_6}{R^6} - \frac{C_8}{R^8} - \frac{C_{10}}{R^{10}} - \frac{C_{12}}{R^{12}}$ (with $C_6 = 269.236a_0^6$, $C_8 = -2803.36a_0^8$, and $C_{10} = 5.786a_0^{10}$, $C_{12} = -7008.84\ a_0^{12}$), is supplemented with the short-range repulsive Born-Mayer potential $A_{eff}e^{(-bR)}$ (with A = 36.9435 hartree and b = $1.71661a_0^{-1}$) and the polarization contribution: $-\frac{2\alpha_{He}}{R^4}$ with $\alpha_{He} = 1.3834a_0^3$.[30]

While the ELJ potential model is expressed as follows

$$V_{ELJ}(R) = \sum_{i=0}^{6} \frac{C_{2i+4}}{R^{2i+4}}$$

(with $C_4 = 2.76a_0^4$, $C_6 = -560.939a_0^6$, $C_8 = 23430.3a_0^8$, and $C_{10} = -414934a_0^{10}$,$C_{12} = 3.5419 \times 10^6 a_0^{12}$, $C_{14} = 5.53833 \times 10^6 a_0^{14}$ and $C_{16} = -1.86459 \times 10^8 a_0^{16}$).

In Figure 1, we compare the original numerical CCSD (T) with the TT and ELJ analytical fitted potentials. To quantify and evaluate the quality of the fitting, we have calculated the root-mean-square error (RMSE) detailed in ref[31] for the TT

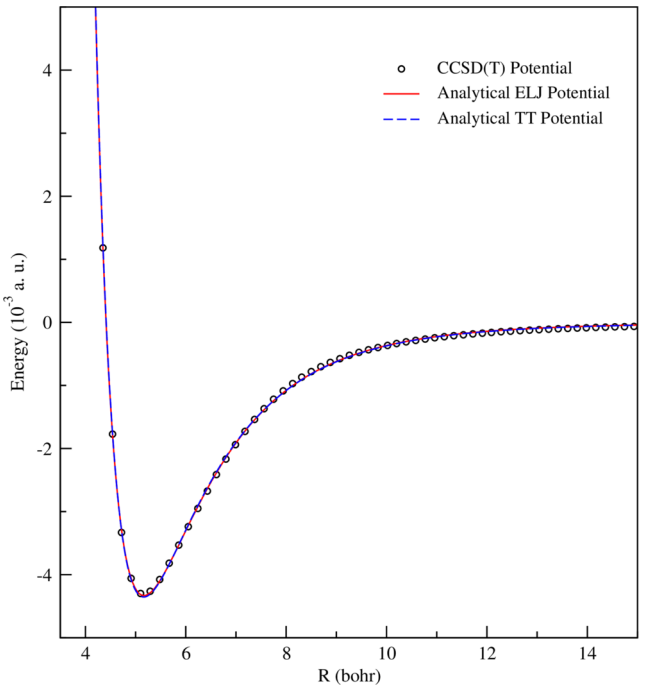

Figure 1. Numerical CCSD(T) $Sr^{2+}He$ PEC compared to TT and ELJ analytical potential fitting ones.

https://doi.org/10.1021/acsomega.4c01433
ACS Omega 2024, 9, 32604−32616

Table 1. Spectroscopic Constants: Equilibrium Distance R_e, Potential Well Depth D_e, Vibrational Constant ω_e, Anharmonic Constant $\omega_e\chi_e$, and Rotational Constant B_e of the Ground State of $Sr^{2+}He$ Compared with Available Results

R_e (bohr)	D_e (cm^{-1})	ω_e (cm^{-1})	$\omega_e\chi_e$ (cm^{-1})	B_e (cm^{-1})	method/basis: Sr/He	refs
5.16	946	209	11.5	0.590	CCSD(T)/d-aug-cc-PV5Z	this work
5.16	956	215	18.3	0.591	TT-Fit	this work
5.17	951	210	17.9	0.590	ELJ-Fit	this work
5.19	914	224	12.8	0.678	RCCSD(T)/ECP28MDF_aV5Z/aug-cc-pV5Z	9

and ELJ interpolations. The Root Mean Square (RMSE) error is computed as follows: $\sqrt{\frac{\sum_{k=1}^{N_p}(V_k^{fit}-V_k^{ab\text{-}initio})^2}{N_p}}$, where N_p represents the number of ab initio points. V_k^{fit} and $V_k^{ab\ initio}$ denote the analytical and numerical potentials, respectively.

To assess the adequacy of the potential energy curves for the ground state of $Sr^{2+}He$ and their fitting in both analytical forms, we compare the derived spectroscopic parameters with those presented in the literature. In Table 1, we initially compare our CCSD(T) spectroscopic constants with those reported by Gardner et al.[9] A favorable agreement is observed for R_e and D_e, indicating that the basis sets are indeed versatile and capable of depicting the interactions within the $Sr^{2+}He$ ionic molecular system.

Second, we compare the fitted potentials with the original one (CCSD(T)) using the root mean squares (RMSEs) and their spectroscopic constants. The fitting of the CCSD(T) original potential yields reasonable RMSEs values: 1.912×10^{-5} and 1.666×10^{-5} a.u. for the TT and ELJ analytical potentials, respectively. We observe that both fittings accurately reproduce the original CCSD(T) potential. However, the ELJ potential provides a better description for the well depth, with a difference of only 5 cm^{-1}, compared to about 10 cm^{-1} for the TT potential. The equilibrium distance for TT is exactly the same as the CCSD(T) value, whereas ELJ differs by only 0.01 bohr. Consequently, we utilize both analytical forms, as this aids in their analysis across all interaction distance ranges and enables the study of the effects of these small differences on excited states, which may have equilibrium distances at internuclear positions different from that of the $Sr^{2+}He$ ground state.

2.2. Electron-$Sr^{2+}He$ Interaction ($V_{e-Sr^{2+}He}$). For the $V_{e\text{-}SrHe}{}^{2+}$ interaction, we conducted a single-electron ab-intio self-consistent field (SCF) computation, wherein the $[Sr^{2+}]$ core and the electron-helium effects were replaced with semilocal pseudopotentials. The pseudopotentials, as suggested by Barthelat and Durand,[32] are employed to confine the active electrons to only valence electrons in the ionic Sr^+He and neutral SrHe systems. The core polarization pseudopotentials, denoted as V_{CCP}, have been integrated into the framework using the l-dependent development of Foucrault et al.,[33] which extends the initial approach proposed by Müller and Meyer.[34] These pseudopotentials account for the polarization effects on both the alkaline ionic cores and the helium atom as a whole. For each atom, whether it is strontium (λ = Sr) or helium (λ = He), the core polarization effects are quantified and described using an effective potential.

$$V_{CPP} = -\frac{1}{2}\sum_{\lambda}\alpha_\lambda \vec{f}_\lambda \vec{f}_\lambda$$

α_λ signifies the electric dipole polarizability of the atomic core λ, and $\vec{f}_\lambda$ represents the electric field created at center λ produced by the valence electrons and all other atomic cores.

For Helium and Strontium, the values of polarizabilities were taken as $\alpha_{He} = 1.3834a_0^3$ and $\alpha_{Sr^{2+}} = 5.67a_0^3$, respectively, from refs 30,35. The cutoff radius has been fine-tuned specifically for the strontium (Sr) atom to match and replicate the energy level spectrum observed in experimental data as documented in ref 36. The computed ionization potential (IP) and the energy differences for the lowest atomic energy levels from the ground state are provided for both Sr^+ and Sr in Table 2[37]. We employed the identical uncontracted (3s2p) basis set for the He atom of ref 38.

Table 2. Calculated and Observed IPs and Atomic Transitions for Atomic Sr^+ and Sr

	this work (cm^{-1})	exp (cm^{-1})[36]	ΔE (cm^{-1})
IP (5s)	−88963.97	−88965.70	1.73
5s−4d	−74267.92	−74241.47	26.45
5s−5p	−64848.06	−64716.02	132.04
5s−6s	−41178.55	−41228.79	50.24
5s−5d	−35371.90	−35626.98	255.08
5s−6p	−33020.89	−33003.42	17.47

Employing a basis set for the helium (He) atom is crucial for addressing the geometric deformation of the strontium (Sr) valence orbitals. This distortion arises from their need to remain orthogonal to the rare-gas (RG) closed shells, represented by pseudopotentials. As there are no active electrons on the helium atom, the exponents were carefully determined to ensure the proper overlap with the 3s and 2p orbitals of helium and to extend into the diffuse range as required. The electron-helium (e-He) effects have been replaced by semi local pseudopotentials. The pseudopotential parameters were developed in detail in our previous study on Mg^+He.[19] Regarding the interaction of two valence electrons and $Sr^{2+}He$, which is necessary for the SrHe neutral system, in addition to the SCF calculations, full CI calculations are performed, and the energy will be added to the Sr^{2+}-He fitted potentials.

2.3. Spin−Orbit Coupling (V_{SO}). The spin−orbit effect is incorporated into both systems, the ionic Sr^+He and the neutral SrHe, using the semi empirical scheme of Cohen and Schneider.[39]

The spin−orbit coupling matrices of the Sr^+He states dissociating into Sr^+(5p, 6p (Ω = 3/2, 1/2))+He, and Sr^+(4d, 5d (Ω = 5/2, 3/2, 1/2))+He; and those of the SrHe, dissociating into Sr(5s5p (Ω = 2, 1, 0^+, 0^-))+He and Sr(5s4d(Ω = 0^-; 0^+; 1; 2; 3))+He, exhibit isomorphism with matrices provided by Cohen and Schneider[39] for the $2p^5$ and $2p^53s$ configuration of Ne^+ and Ne*, respectively. Detailed matrices for the np and nd configurations can be found in refs 20−26. The corresponding spin−orbit constants, ξ, are derived from the atomic spectra of the NIST database.[36]

https://doi.org/10.1021/acsomega.4c01433
ACS Omega 2024, 9, 32604−32616

3. RESULTS AND DISCUSSION

3.1. Sr^+He: Without Spin−Orbit Coupling. For the Sr^+He ionic system, we determined a total of 12 potential energy curves (PECs) for electronic states: 6 of $^2\Sigma^+$, 4 of $^2\Pi$ and 2 of $^2\Delta$ symmetries. These states are asymptotically correlated to the lowest lying atomic ^2S, ^2P and ^2D states of the Strontium atom.

The potential energy curves are presented in Figure 2, and their spectroscopic constants are shown on Table 3 To assess

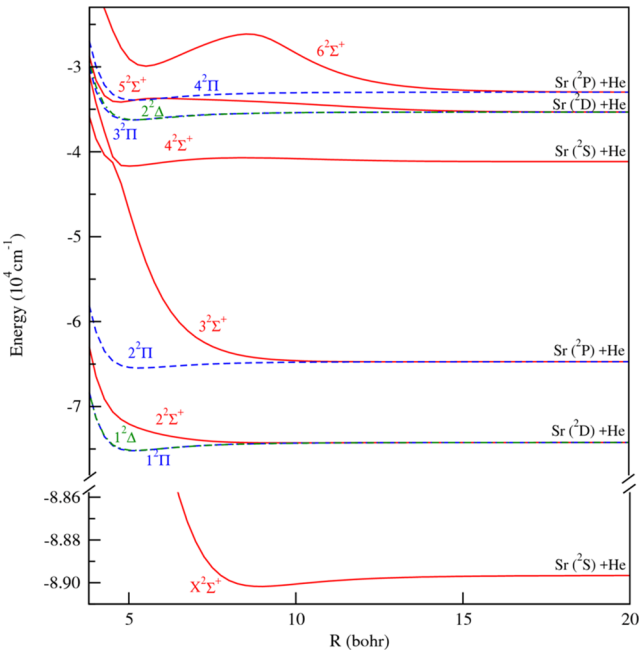

Figure 2. Potential energy curves (PECs) depicting the dissociation of ground and excited electronic states into Sr^+(5s, 4d, 5p, 6s, 5d and 6p) + He.

the quality and accuracy of our calculations, these curves are utilized to extract the spectroscopic parameters (R_e, D_e, ω_e, $\omega_e\chi_e$, T_e, and B_e) from their numerical potential energy curves.

As anticipated, a large equilibrium distance of R_e = 8.94(8.91) bohr and a shallow potential well of D_e = 53(49) cm^{-1} are observed for the ELJ-Fit (TT-Fit) for the ground electronic state $X^2\Sigma^+$ of the molecular ionic dimer Sr^+He, which is considered here as a one-electron system. This is associated with the typical classical van der Waals bonding for this molecular ion. In fact, the equilibrium distances found for both ELJ and TT fittings are almost the same, while the well depths differ by 4 cm^{-1}, which is nearly the difference between the ELJ and TT fittings for the $Sr^{2+}He$ ground state. We note that the equilibrium distance (R_e = 7.6 bohr) reported in ref 12 is underestimated compared to all our results as well as that of ref 9 (R_e = 8.59 bohr); however, their well depth (D_e = 48 cm^{-1}) is in excellent agreement with our D_e = 49(53) cm^{-1} using the TT and ELJ analytical potentials.

For the $2^2\Sigma^+$, $1^2\prod$ and $1^2\Delta$states dissociating into Sr^+(4d)+He asymptotic limit, we present our TT and ELJ results, which are compared with those of Massimo and Cagnomi. We obtained almost the same spectroscopic constants for R_e and D_e when using TT and ELJ potentials, except for the $2^2\Sigma^+$ state where a difference of 5 cm^{-1} is observed between the TT (D_e = 41 cm^{-1}) and ELJ (D_e = 45 cm^{-1}) well depths. This difference could be related to the original interpolations of the Sr^{2+} He potential; where the difference at similar internuclear distance is of that order. Compared to the results of Massimo and Cagnomi, there is generally good agreement for the equilibrium distances. However, our D_e for all these states ($2^2\Sigma^+$, $1^2\prod$ and $1^2\Delta$) are overestimated compared to the results found by Massimo and Cagnomi. The differences between our and theirs are approximately 20 cm^{-1} for $2^2\Sigma^+$, 370 cm^{-1} for $2^2\prod$ and 643 cm^{-1} for $1^2\Delta$, respectively.

For the $3^2\Sigma^+$ and $2^2\prod$ excited states, which correlate with Sr^+(5p) + He asymptotic limit, the potential energy curves (PECs) and spectroscopic constants are presented, respectively, in Figure 2 and Table 2. As shown in Table 2, the agreement with Massimo and Cagnomi[8] for R_e is reasonably good, with values of 12.93 bohr compared to 13.45 (13.24) bohr. The difference is 0.49 and 0.35 bohr with our TT and ELJ potentials, respectively. However, the agreement is good between our D_e (5 and 6 cm^{-1}) with Massimo and Cagnomi, who found a well depth of 4.7 cm^{-1}.

The spectroscopic constants of the higher excited states of $^2\Sigma^+$, $^2\prod$ and $^2\Delta$ symmetries dissociating into Sr^+(6s, 5d, and 6p) + He are also gathered in Table 3. Since we do not have comparisons for these states, we present only our results with TT and ELJ fittings for $Sr^{2+}He$. As can be seen in Table 3, the difference between the TT and ELJ results does not exceed 0.01 bohr for R_e and approximately 2 cm^{-1} for D_e. The PECs of these states without spin−orbit are shown in Figure 2. As expected, states of $^2\prod$ and $^2\Delta$ symmetries present relatively deep well depths of hundreds of cm^{-1} located at short distances, in contrast to the $^2\Sigma^+$ states, which are weakly bound ($D_e \approx 10$ of cm^{-1}), or repulsive with barriers at large internuclear distances. However, the $4^2\Sigma^+$(6s) state makes an exception with a short equilibrium distance (R_e = 4.93 bohr) and a relatively deep well of D_e = 540 cm^{-1}.

Indeed, at higher energies, strong interactions between states dissociating into the close-lying 5p and 6s asymptotic configurations are evident. This results in a short distance avoided crossing between the $3^2\Sigma^+$ and $4^2\Sigma^+$ states as they dissociate to the Sr^+(5p) + He and Sr^+(6s) + He limits, explaining the short equilibrium distance of the $4^2\Sigma^+$(6s) state. The $6^2\Sigma^+$ state presents a remarkably interesting profile, featuring a low minimum followed by an extended barrier that will trap metastable levels.

3.2. Sr^+He: Spin−Orbit Coupling for ^2P and ^2D States. In this section, we present the PECs and spectroscopic constants of the first and higher excited states with $^2\Sigma^+$, $^2\prod$ and $^2\Delta$ symmetries, determined through spin−orbit coupling. The spin−orbit coupling constants utilized in the calculation are taken from the NIST database[36] as follows: $\xi_{5p}(Sr^+)$ = 801.46 cm^{-1}, $\xi_{6p}(Sr^+)$ = 288.2 cm^{-1}, $\xi_{4d}(Sr^+)$ = 280.34 cm^{-1} and $\xi_{5d}(Sr^+)$ = 86.66 cm^{-1}. Figures 3 and 4 show the behavior of the $Sr^+(^2P)$ + He potential energy curves, incorporating spin−orbit coupling between the ^2P states. They are labeled as $3^2\Sigma_{1/2}^+$, $2^2\Pi_{1/2}$, $2^2\Pi_{3/2}$, $6^2\Sigma_{1/2}^+$, $4^2\Pi_{1/2}$, and $4^2\Pi_{3/2}$. These curves are obtained through diagonalization of the spin−orbit coupling matrix considered as a perturbation and their related spectroscopic parameters are listed in Table 4.

As evident, the quantitative characteristics of energy curves and spectroscopic parameters are significantly influenced by the spin−orbit coupling constants ξ. Specifically, the molecular splitting of $2^2\Pi_{1/2}$ and $2^2\Pi_{3/2}$ components at equilibrium is found to be 238 cm^{-1} for both TT and ELJ potentials. The vibrational constant and equilibrium distance exhibit minor

https://doi.org/10.1021/acsomega.4c01433
ACS Omega 2024, 9, 32604−32616

Table 3. Spectroscopic Constants of the Electronic States of Sr^+He van der Waals System without Spin-Orbit Coupling

state	R_e (bohr)	D_e (cm^{-1})	T_e (cm^{-1})	ω_e (cm^{-1})	$\omega_e\chi_e$ (cm^{-1})	B_e (cm^{-1})	refs
$X^2\sum^+(5s)$	8.91	49		36.38	6.75	0.198664	TT-Fit
	8.94	53		39.54	7.37	0.197036	ELJ-Fit
	8.59	28.9		21.1	4.12	0.220	9
	7.6	48					12
$3^2\sum^+(5p)$	13.45	5	24,297				TT-Fit
	13.24	6	24,291				ELJ-Fit
	12.93	4.7					8
$2^2\Pi(5p)$	5.31	746	23,551	180.64	14.89	0.558530	TT-Fit
	5.30	747	23,550	182.70	15.40	0.559719	ELJ-Fit
	4.91	683					8
$2^2\sum^+$ (4d)	9.68	41	14,740	20.56	2.57	0.167891	TT-Fit
	9.66	45	14,736	22.82	2.89	0.168589	ELJ-Fit
	11.15	19					8
$1^2\Pi(4d)$	5.12	973	13,807	222.09	17.78	0.599447	TT-Fit
	5.12	975	13,806	224.07	17.97	0.600056	ELJ-Fit
	4.80	603					8
$1^2\Delta(4d)$	5.17	930	13,851	206.34	16.96	0.587766	TT-Fit
	5.17	931	13,849	208.24	17.09	0.588542	ELJ-Fit
	5.27	287		138.20	22.12	0.574289	8
$4^2\sum^+(6s)$	4.93	541	47,316	385.81	152.29	0.658968	TT-Fit
	4.93	543	47,314	384.58	159.10	0.658886	ELJ-Fit
$5^2\sum^+(5d)$	4.69[a]	−1164	54,856				TT-Fit
	4.69[a]	−1162	54,854				ELJ-Fit
$3^2\Pi(5d)$	5.05	951	52,741	227.82	18.80	0.617395	TT-Fit
	5.05	953	52,739	229.74	18.84	0.617818	ELJ-Fit
$2^2\Delta$ (5d)	5.19	920	52,772	204.62	15.94	0.585226	TT-Fit
	5.18	921	52,771	206.67	16.23	0.586046	ELJ-Fit
$6^2\sum^+(6p)$	5.49[a]	−3054	59,089				TT-Fit
	5.49[a]	−3054	59,089				ELJ-Fit
$4^2\Pi$ (6p)	5.18	947	55,089	211.89	16.32	0.586704	TT-Fit
	5.18	948	55,088	213.78	16.51	0.587457	ELJ-Fit

[a]Potential barrier.

adjustments, whereas the excitation energy T_e is heavily influenced, primarily due to a substantial spin−orbit splitting of approximately 823 cm^{-1}.

Additionally, the potential well of the $2^2\Pi_{1/2}$ state of $Sr^+(^2P_{1/2})$ + He, with its depth diminishing to 367 (368) cm^{-1} from the original 746 (747) cm^{-1} in the $^2\Pi$ states respectively for TT and ELJ fittings, exhibits a low entrance barrier on the corresponding energy curve. Furthermore, it is observed that the well of the $2^2\Pi_{3/2}$, dissociating, into $Sr^+(^2P_{3/2})$ + He, remains, significantly unchanged compared to the ab- initio results without spin−orbit interaction. However, both the equilibrium distance and well depth of ref 12. are in disagreement with both our results and those of ref 8. The difference with the ref 12. can be attributed to their utilization of different pseudopotentials and limited basis sets in their calculations.

Furthermore, the state $3^2\sum^+$ correlated to the $Sr^+(5p)$ + He limit is also investigated, incorporating spin−orbit coupling. The $3^2\sum_{1/2}{}^+$ state is characterized by a shallow potential well with a depth of D_e = 9 (10) cm^{-1} localized at R_e = 12.69 (12.48) bohr, which aligns well with the findings of refs 8,12.

A similar situation is found for $Sr^+(6^2P_{1/2})$ + He and $Sr^+(6^2P_{3/2})$ + He limits. Specifically, the potential well of the $4^2\Pi_{1/2}$ state decreases to 818 (813) cm^{-1} from the original $4^2\Pi$ states depth of 947 (948) cm^{-1}. Additionally, it is noted that the well depth of the $4^2\Pi_{3/2}$, dissociating into $Sr^+(^2P_{3/2})$ + He, remains nearly unaffected compared to the original depth obtained without spin−orbit coupling. It is important to mention that the potential energy curve of $6^2\sum_{1/2}{}^+$ exhibits a notable barrier due to the repulsive interaction between the electron and the He atom.

In Figure 5, potential energy curves are displayed for the states dissociating into $Sr^+(4^2D_{1/2}$, $4^2D_{3/2}$ and $4^2D_{5/2})$ atomic limits, which arise from considering spin−orbit interaction for the Sr^+(4d) + He molecular system. It is observed that the equilibrium distances and well depths of these states are slightly affected. However, the transition energy T_e, undergoes shifts of 294, 73, 141, 531, and 280 cm^{-1}, respectively, for the $3^2\sum_{1/2}{}^+$, $2^2\Pi_{1/2}$, $2^2\Pi_{3/2}$, $1^2\Delta_{3/2}$, and $1^2\Delta_{5/2}$ states.

For the $5^2D_{1/2}$, $5^2D_{3/2}$ and $5^2D_{5/2}$, atomic terms arising from $Sr^+(5d)$ limit, five electronic states including spin−orbit interaction are generated and presented in Figure 6. Analogously, we encounter a comparable situation with states dissociating into $Sr^+(4^2D_{1/2}$, $4^2D_{3/2}$, and $4^2D_{5/2})$ atomic levels. Nevertheless, the impact is notably more subdued compared to the states dissociating into the $Sr^+(^2P_{1/2})$ + He and $Sr^+(^2P_{3/2})$ + He limits. This disparity can be traced back to the small spin−orbit constant value in the 5d atomic limit.

3.3. SrHe without Spin−Orbit Coupling. Within the model utilized, as detailed in Section 2, the SrHe molecular system is treated as comprising only two valence active electrons interacting with Sr^{2+}He ionic dimer. In this context, a full configuration interaction (CI) calculation is conducted to derive accurate potential energy curves for the two-electron

https://doi.org/10.1021/acsomega.4c01433
ACS Omega 2024, 9, 32604−32616

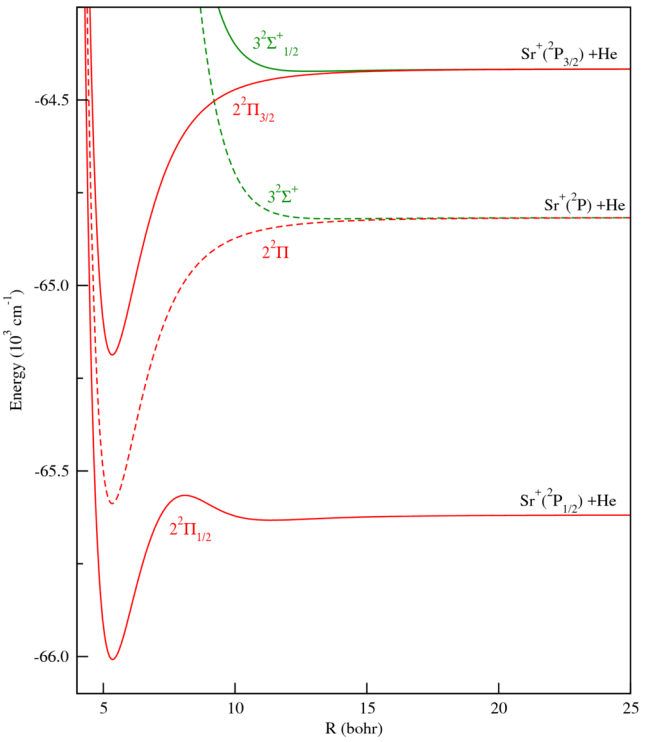

Figure 3. PECs including spin−orbit coupling for Sr^+ ($5\ ^2P$) + He. Solid lines represent states including spin−orbit coupling, and dashed lines represent states without spin−orbit coupling.

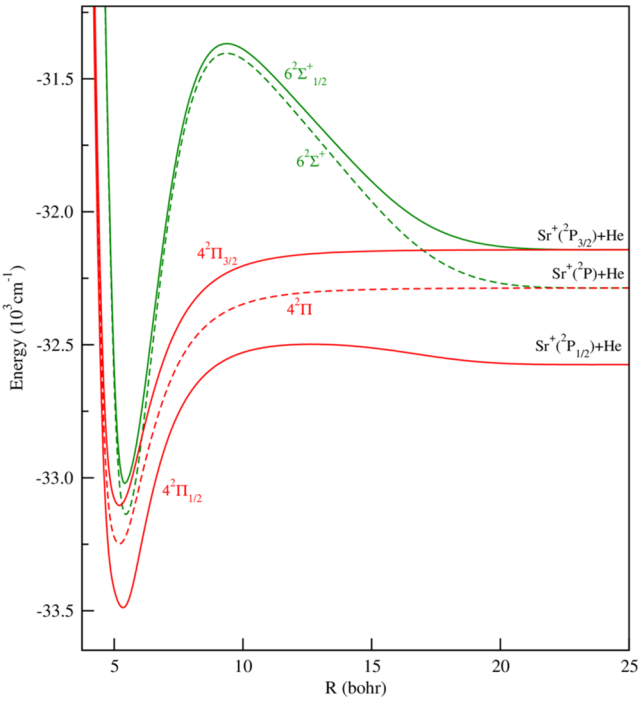

Figure 4. PECs including spin−orbit coupling for Sr^+ ($6\ ^2P$) + He. Solid lines represent states including spin−orbit coupling, and dashed lines represent states without spin−orbit coupling.

system within the model. To assess and validate the reliability of the model applied to SrHe, we determined the spectroscopic constants of the molecular electronic states dissociating into Sr ($5s^2$, 5s5p, 5s5d and 5s6s) + He limits. The potential energy curves of these states are depicted in Figure 7, and the corresponding spectroscopic parameters are presented in Table 5 As evident from Table 5, the ground state $1^1\sum^+$ exhibits a remarkably shallow well, with a depth of only 3 cm^{-1}. Lovallo and Klobukowski[14] conducted CCSDT calculations for the ground state and reported both nonrelativistic and scalar-relativistic results (D_e and R_e), which are included in Table 5 for comparison. The scalar-relativistic values are provided within parentheses. It is noteworthy that our result for D_e (3 cm^{-1}) aligns excellently with the calculations by Lovallo and Klobukowski,[14] who reported values of 2.85 (and 2.96 cm^{-1}) from the two levels of calculations, respectively. However, a generally good agreement is observed for R_e, with a difference of approximately 0.33 bohr. According to Yin et al.,[15] the ground state presents a small well depth calculated from the fitted TT model potentials using two series of dispersion coefficients for n_{max} = 5 (and for n_{max} = 8), as presented in the Table 5.

Furthermore, the current results are compared with the multireference configuration interaction MRCI results of Stienkemeier et al.[7] and the integral surface results of Kleinekathöfer.[10] It is noted that their well depths are greater (7.11 and 12.71 cm^{-1}, respectively), and the equilibrium distances are shorter (10.47 and 10.79 bohr, respectively) than our current values. The general good agreement observed between our calculations and those of Lovallo and Klobukowski[14] and Yin et al.,[15] for both R_e and D_e, validates the used model, considering the varying repulsive nature of the ground state. Indeed, within the limits of accuracy of ab -initio calculations, we can assert a general consensus regarding the ground state among all references and our calculations, despite the simplicity of the model utilized for SrHe van der Waals molecular system. As there are no available studies for the excited states, we solely present our predicted results. Generally, we observe that the excited states of the neutral system SrHe tend to be predominantly repulsive, although some exhibit shallow wells at large equilibrium distances.

3.4. SrHe with Spin−Orbit Coupling for ^{1,3}P and ^{1,3}D states. Considering the influence of the spin−orbit effect in the SrHe van der Waals system, we depict the potential energy curves for eight electronic states in Figures 8 and 9. These states correspond to $\Omega = 0^-$ and 0^+ for the former, and Ω = 1, 2, 3 with 7, 4, 1 state, respectively. The associated spectroscopic constants are provided in Table 6. These values are presented here for the first time, and therefore, there is no comparison with other results, with most of them being repulsive. For these states, it is noticeable that the (1) $^3\Pi$ state splits into four states: $(1)^3\Pi_{0-}$, $(1)^3\Pi_{0+}$, $(1)^3\Pi_1$ and $(1)^3\Pi_2$. Additionally, the primary discrepancy among their spectroscopic constants, lies in T_e, where the energy splitting between the upper and lower states is approximately 574 cm^{-1}. It is observed that these effects for the excited states Sr ($5s4d^{1,3}D$) + He ($(2)^{1,3}\Sigma^+$, $(2)^{1,3}\Pi$ and (1) $^{1,3}\Delta$) are considerably smaller than those observed for the states dissociating into Sr ($5s5p\ ^3P_{0,1,2}$) + He and Sr($5s5p\ ^1P_1$)+He limits, attributed to the relatively modest spin−orbit constant for the 4d atomic limit (ξ_{4d} = 59.74 cm^{-1}).

3.5. Permanent and Transition Dipole Moments for Sr^+He and SrHe van der Waals Systems. The permanent and transition dipole moments (PDM and TDM) are crucial pieces data for various physical phenomena. In this context, we have calculated the permanent and transition dipole moments for all electronic states of the molecular ion Sr^+He and neutral SrHe, considering one and two valence electrons, respectively.

https://doi.org/10.1021/acsomega.4c01433
ACS Omega 2024, 9, 32604−32616

Table 4. Spectroscopic Constants of the Electronic States of Sr^+He van der Waals System Including Spin-orbit Coupling for Sr^+ ($5\ ^2P$) + He, Sr^+ (6^2P) + He, Sr^+ ($4\ ^2D$) + He and Sr^+ ($5\ ^2D$) + He

state	R_e (bohr)	D_e (cm^{-1})	T_e (cm^{-1})	ω_e (cm^{-1})	$\omega_e\chi_e$ (cm^{-1})	B_e (cm^{-1})	refs
$3^2\sum_{1/2}^+(5p)$	12.69	9	24,689				TT-Fit
	12.48	10	24,687				ELJ-Fit
	12.93	4.7					8
	10.3	16					12
$2^2\Pi_{1/2}(5p)$	5.33	367	23,128	174.36	16.31	0.554977	TT-Fit
	11.21	18	23,477				TT-Fit
	5.32	368	23,128	176.45	16.76	0.556226	ELJ-Fit
	11.09	21	23,475				ELJ-Fit
	4.91	430					8
	9.0	24					12
$2^2\Pi_{3/2}(5p)$	5.31	746	23,951	180.63	14.87	0.558524	TT-Fit
	5.30	747	23,951	182.69	15.38	0.559712	ELJ-Fit
	4.91	679					8
	5.8	217					12
$2^2\sum_{1/2}^+(4d)$	8.58	86	15,034	41.40	8.51	0.213362	TT-Fit
	8.59	87	15,031	41.38	9	0.213201	ELJ-Fit
	10.3	16					12
$1^2\Pi_{1/2}(4d)$	5.15	735	13,880	211.08	18.39	0.592159	TT-Fit
	5.15	736	13,878	213.10	18.57	0.592886	ELJ-Fit
$1^2\Pi_{3/2}(4d)$	5.12	**973**	13,948	222.09	17.78	0.599447	TT-Fit
	5.12	975	13,946	224.05	17.95	0.600056	ELJ-Fit
$1^2\Delta_{3/2}(4d)$	5.16	869	13,320	210.93	17.72	0.591905	TT-Fit
	5.15	871	13,318	212.94	17.92	0.592634	ELJ-Fit
$1^2\Delta_{5/2}(4d)$	5.17	930	14,131	206.33	16.95	0.587765	TT-Fit
	5.17	931	14,130	208.24	17.09	0.588543	ELJ-Fit
$5^2\sum_{1/2}^+(5d)$	4.69[a]	−1065	54,861				TT-Fit
	4.69[a]	−1064	54,860				ELJ-Fit
$3^2\Pi_{1/2}(5d)$	5.11	861	52,779	224.65	20.00	0.601650	TT-Fit
	5.11	863	52,778	226.62	20.12	0.602226	ELJ-Fit
$3^2\Pi_{3/2}(5d)$	5.05	951	52,784	227.81	18.80	0.617393	TT-Fit
	5.05	953	52,782	229.75	18.85	0.617821	ELJ-Fit
$2^2\Delta_{3/2}(5d)$	5.12	903	52,606	206.85	16.11	0.600322	TT-Fit
	5.12	905	52,604	206.27	13.71	0.600895	ELJ-Fit
$2^2\Delta_{5/2}(5d)$	5.19	920	52,859	204.63	15.94	0.585226	TT-Fit
	5.18	921	52,858	206.67	16.24	0.586047	ELJ-Fit
$6^2\sum_{1/2}^+(6p)$	5.49[a]	−2920	59,099				TT-Fit
	5.48[a]	−2920	59,100				ELJ-Fit
$4^2\Pi_{1/2}(6p)$	5.18	818	54,935	211.71	15.96	0.585994	TT-Fit
	5.18	813	54,934	213.55	16.12	0.586748	ELJ-Fit
$4^2\Pi_{3/2}(6p)$	5.18	947	55,233	211.88	16.32	0.586703	TT-Fit
	5.18	948	55,232	213.78	16.51	0.587456	ELJ-Fit

[a]Potential barrier.

For Sr^+He, the associated transition dipole moments $^2\sum^+ \rightarrow {}^2\Pi$ and $^2\sum^+ \rightarrow {}^2\sum^+$, pertaining to transitions originating from the ground state, $X^2\sum^+$, to the first excited states, are calculated while considering the spin−orbit effect. Incorporating this effect necessitates the utilization of the rotational matrix derived from the diagonalization of the energy matrix discussed previously.

The results of the TDMs with and without spin−orbit are presented in Figure 10. It is noteworthy that the $X^2\sum^+ \rightarrow 3^2\sum^+$ transition exhibits a maximum of 2.119 bohr, located at R = 10.71 bohr. At large distances, both the $X^2\sum^+ \rightarrow 3^2\sum^+$ and $X^2\sum^+ \rightarrow 2^2\Pi$ transitions tend toward a pure atomic transition $Sr^+(5s) \rightarrow Sr^+(5p)$. In the same figure, the TDMs are depicted with the inclusion of spin−orbit interaction. It is evident that the $X^2\sum^+ \rightarrow 2^2\Pi$ transition moment splits into two curves associated with the $X^2\sum^+ \rightarrow 2^2\Pi_{1/2}$ and $X^2\sum^+ \rightarrow 2^2\Pi_{3/2}$ transitions. The difference between the split TDMs is remarkable at intermediate distances. At the asymptotic limits, the $X^2\sum^+ \rightarrow 2^2\Pi_{1/2}$, $X^2\sum^+ \rightarrow 2^2\Pi_{3/2}$ and $X^2\sum^+ \rightarrow 3^2\sum_{1/2}^+$ transitions tend toward the $Sr^+(5s) \rightarrow Sr^+(5p)$ pure atomic transition.

Furthermore, the PDMs and TDMs of the neutral SrHe system are also of significant importance. They can furnish experimentalists with vital information for measuring rotationally resolved absorption spectra in alkaline earth/rare gas and alkaline/rare gas complexes. For this end, dipole moment curves have been evaluated for various internuclear separations ranging from 3 to 200 bohr, enabling analysis of their behaviors at short and long distances. The PDMs and TDMs curves are collected in Figures 11 and 12, respectively, for the electronic states of $^{1,3}\sum^+$, $^{1,3}\Pi$ and $^{1,3}\Delta$ symmetries.

https://doi.org/10.1021/acsomega.4c01433
ACS Omega 2024, 9, 32604−32616

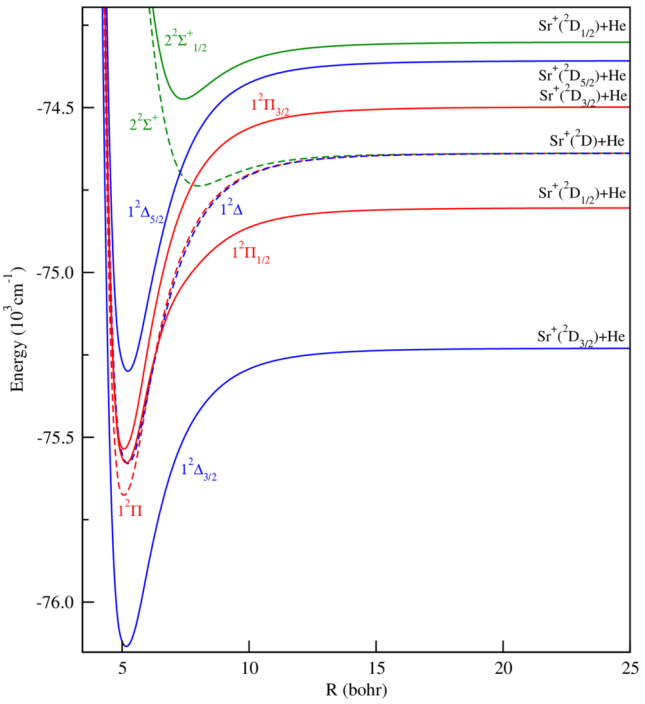

Figure 5. PECs including spin−orbit coupling for Sr^+ ($4\ ^2D$) + He. Solid lines represent states including spin−orbit coupling, and dashed lines represent states without spin−orbit coupling.

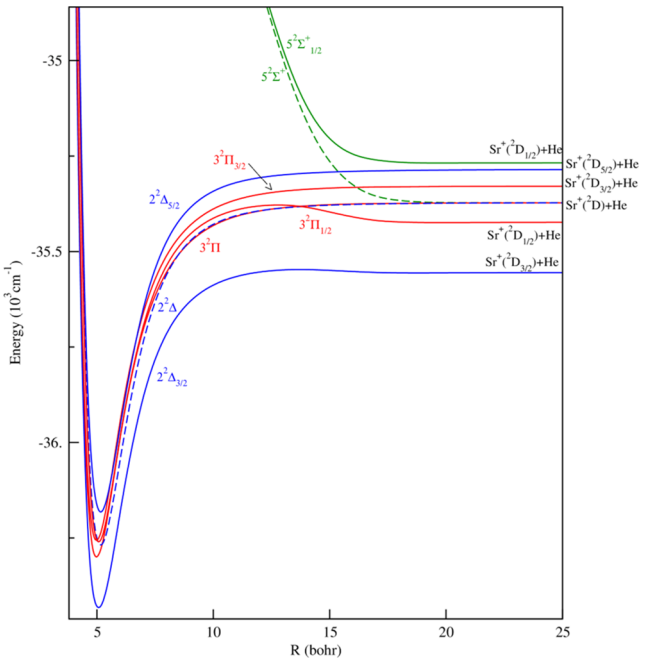

Figure 6. PECs including spin−orbit coupling for Sr^+ ($5\ ^2D$) + He. Solid lines represent states including spin−orbit coupling, and dashed lines represent states without spin−orbit coupling.

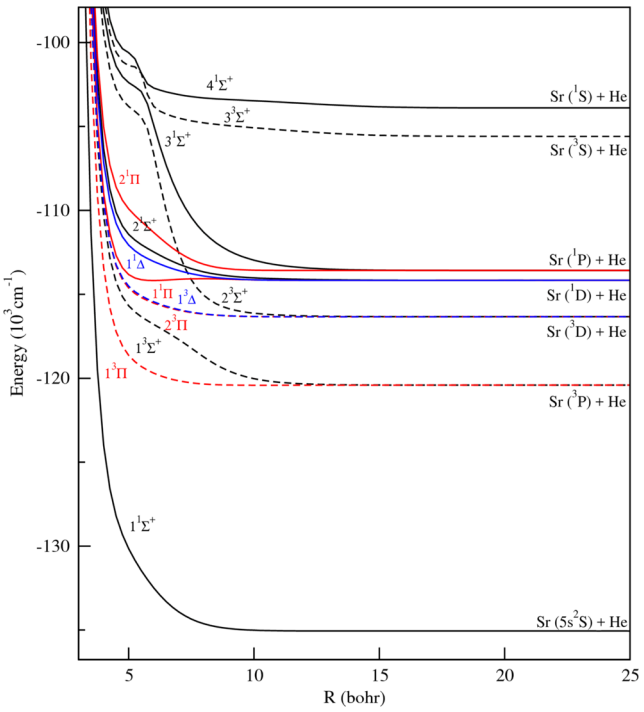

Figure 7. PECs of the ground and excited electronic states corresponding to Sr(5*s*2, 5*s*5*p*, 5*s*4*d* and 5*s*6*s*)+He.

Table 5. Spectroscopic Constants of Molecular States in $^{1,3}\Sigma^+$, $^{1,3}\Pi$ and $^{1,3}\Delta$ Symmetries of SrHe Neutral System

state	R_e (bohr)	D_e (cm^{-1})	T_e (cm^{-1})	refs
$1^1\Sigma^+$	12.49	3		ELJ
	repulsive			TT
	12.13[a] (11.9[b])	2.85[a](2.96[b])		14
	9.81[c](9.68[d])	9.77[c](11.45[d])		15
	10.47	7.11		10
	10.79	12.71		7
$2^1\Sigma^+$	repulsive			this work
$3^1\Sigma^+$	repulsive			this work
$4^1\Sigma^+$	repulsive			this work
$1^3\Sigma^+$	repulsive			this work
$2^3\Sigma^+$	repulsive			this work
$3^3\Sigma^+$	repulsive			this work
$1^1\Pi$	5.97	12	20,880	this work
$2^1\Pi$	12.91	2	21,477	this work
$1^3\Pi$	10.44	7	14,639	this work
$2^3\Pi$	11.89	4	18,718	this work
$1^1\Delta$	13.30	3	20,890	this work
$1^3\Delta$	12.32	4	18,718	this work

[a]Scalar Relativistic SR. [b]Non Realtivistic NR calculations. [c]two sets of parameters A and b for the TT potential, n_{max} = 5; [d]two sets of parameters A and b for the TT potential n_{max} = 8

As presented in Figure 11, the PDMs change the sign at small internuclear distances (less than 15 bohr). Additionally, it is notable that the PDM of $^3\sum^+$ electronic state exhibits significant variation compared to other electronic states of $^{1,3}\Pi$ and $^{1,3}\Delta$ symmetries. Subsequently, the PDM rapidly diminishes to zero at large distances.

Figure 12 illustrates the TDMs curves for $^{1,3}\Sigma \rightarrow {}^{1,3}\Sigma$ and $^{1,3}\Pi \rightarrow {}^{1,3}\Pi$ molecular transitions. As observed, the most pronounced variations in TDMs are especially notable for the $2^3\Sigma^+ \rightarrow 3^3\Sigma^+$ and $1^3\Pi \rightarrow 1^3\Pi$ transitions, particularly at short and intermediate interatomic distances. The shape of TDMs curves reveals significant peaks at short and intermediate distances, often associated with avoided crossings in the PECs. Conversely, at large internuclear distances, the TDMs either diminish or converge to a constant value, indicating a pure atomic transition.

https://doi.org/10.1021/acsomega.4c01433
ACS Omega 2024, 9, 32604−32616

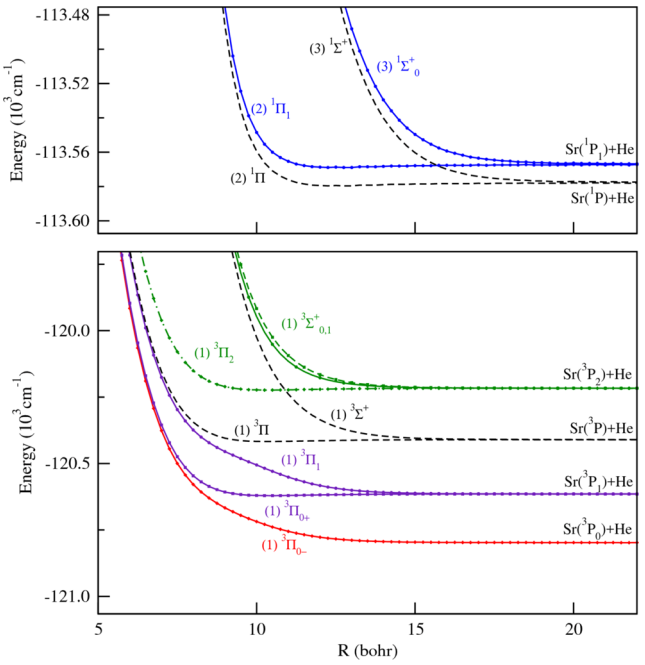

Figure 8. PECs with spin−orbit coupling of SrHe corresponding to Sr (5s5p ^{3}P$_{0-,\,0+,\,1,\,2}$) + He and Sr (5s5p ^{1}P$_{0,1}$) + He. Solid lines + symbol and dashed lines represent states with and without spin−orbit coupling, respectively.

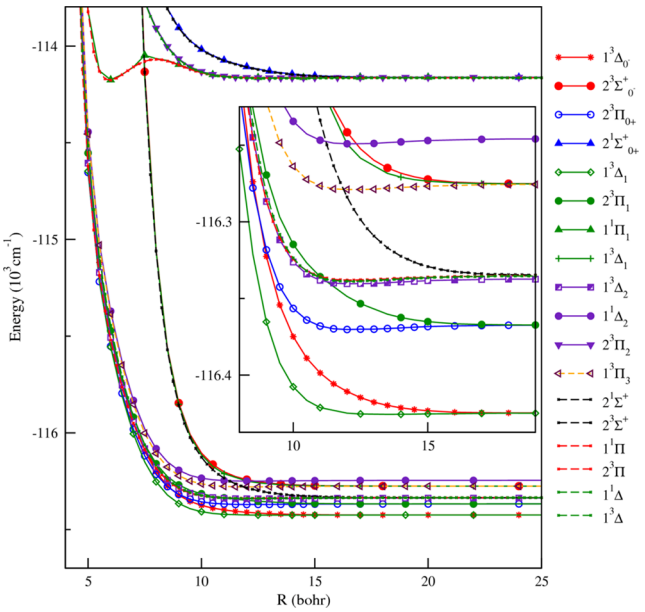

Figure 9. PECs including spin−orbit coupling of SrHe correlating to Sr (5s4d ^{1,3}D$_{0-,0+,1,2,3}$) + He. Solid lines+ symbol represent states with and without spin−orbit coupling, respectively.

3.6. Vibrational Analysis of Sr^+He Introducing the Spin−Orbit Effect.

Theoretical vibrational analysis for excited states of diatomic molecules involves a comprehensive examination of the vibrational behavior beyond the ground state. By employing quantum mechanical principles, such as the Born−Oppenheimer approximation and the harmonic oscillator model, researchers can elucidate the vibrational dynamics of molecules in excited electronic states. This analysis typically involves solving the Schrödinger equation for the molecular Hamiltonian, considering both electronic and vibrational degrees of freedom. Spectroscopic techniques like infrared and Raman spectroscopy play pivotal roles in experimentally verifying these theoretical predictions. Understanding the vibrational behavior in excited states provides valuable insights into molecular structure, reactivity, and energy transfer processes, there by contributing significantly

Table 6. Spectroscopic Constants of Molecular States in $^{1,3}\Sigma^+$, $^{1,3}\Pi$ and $^{1,3}\Delta$ Symmetries of SrHe Neutral System with Spin-Orbit Coupling

molecular state	R_e (bohr)	T_e (cm^{-1})	D_e (cm^{-1})	refs
$(3)^1\sum_0^+$	repulsive			this work
$(2)^1\Pi_1$	12.81	21,487	2	this work
$(1)^3\Sigma_0^+$	10.52	14,435	6	this work
$(1)^3\sum_1^+$	repulsive			this work
$(1)^3\Pi_{0-}$	repulsive			this work
$(1)^3\Pi_{0+}$	repulsive			this work
$(1)^3\Pi_1$	repulsive			this work
$(1)^3\Pi_2$	10.44	14,833	7	this work
$(2)^1\sum_{0+}^+$	repulsive			this work
$(1)^1\Pi_1$	5.95	20,881	13	this work
$(1)^1\Delta_2$	12.05	18,807	4	this work
$(2)^3\sum_{0-}^+$	repulsive			this work
$(2)^3\sum_1^+$	repulsive			this work
$(2)^3\Pi_{0+}$	12.73	18,686	3	this work
$(2)^3\Pi_1$	repulsive			this work
$(2)^3\Pi_2$	13.23	20,892	3	this work
$(1)^3\Delta_{0-}$	repulsive			this work
$(1)^3\Delta_1$	repulsive			this work
$(1)^3\Delta_2$	11.95	18,716	3	this work
$(1)^3\Delta_3$	31.96	18,781	1	this work

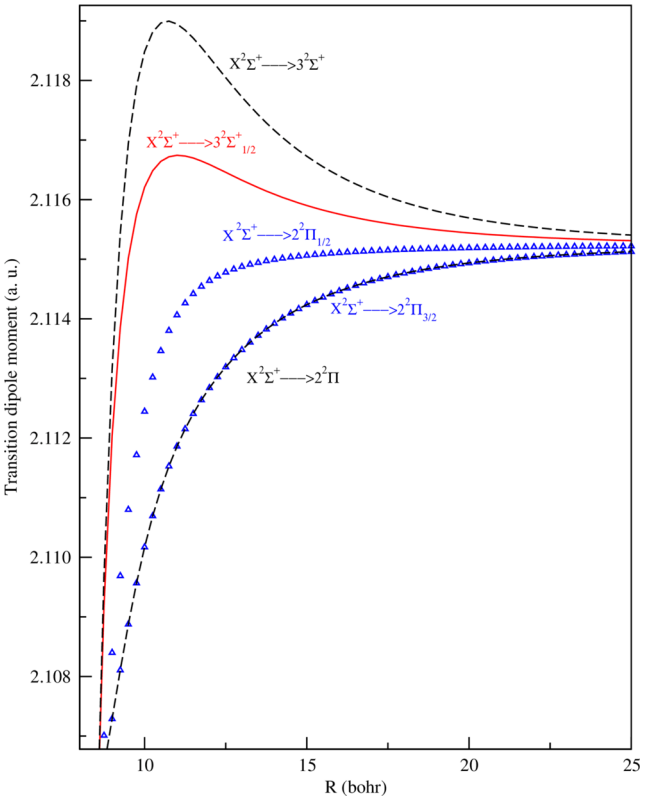

Figure 10. TDMs of $X^2\sum^+ \rightarrow 3^2\Sigma^+$ and $X^2\Sigma^+ \rightarrow {}^{22}\Pi$ with and without spin−orbit coupling of Sr^+He ionic system.

https://doi.org/10.1021/acsomega.4c01433
ACS Omega 2024, 9, 32604−32616

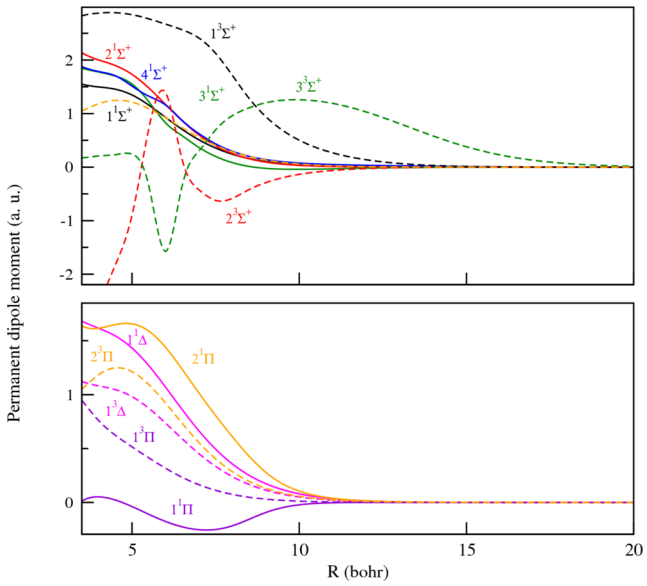

Figure 11. PDMs for ground and excited states in $^{1,3}\sum^{+}$, $^{1,3}\Pi$ and $^{1,3}\Delta$ symmetries of SrHe neutral system.

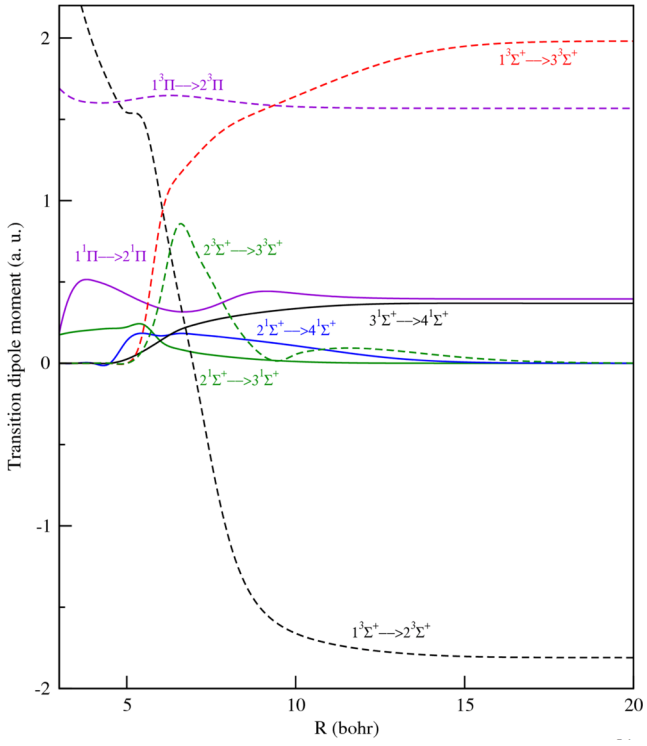

Figure 12. TDMs of $^{1,3}\sum^{+} \rightarrow {}^{1,3}\Sigma^{+}$, $^{1,3}\Pi \rightarrow {}^{1,3}\Pi$ of SrHe neutral system.

to various fields including chemistry, physics, and materials science.

The vibrational energy level spacing $(E_{v+1}-E_v)$ for the ground states ($X^1\sum^{+}$ and $X^2\sum^{+}$) of $Sr^{2+}He$ and $Sr^{+}He$, as well as those of their excited states, have been determined both without and with spin−orbit coupling using the Numerov algorithm.[40−44] They are presented in Tables 7 and 8. We remark that the ground state of the $Sr^{2+}He$ system presents more vibrational levels than $Sr^{+}He$, which can be explained by the difference in the well depths. Specifically, D_e = 946 for $Sr^{2+}He$ ($X^1\sum^{+}$) and D_e = 48 cm^{-1} for $Sr^{+}He$ ($X^2\sum^{+}$). Furthermore, this effect can be observed by comparing the ground $X^2\sum^{+}$ with the $^2\Pi$ and $^2\Delta$states.

Table 8 shows the vibrational level spacings by introducing the spin orbit effect. We found respectively 6, 9, 10, and 11 levels for $\mathbf{2^2\Sigma_{1/2}}^{+}$, $\mathbf{1^2\Pi_{1/2}}$, $\mathbf{1^2\Pi_{3/2}}$, $\mathbf{1^2\Delta_{3/2}}$ and $\mathbf{1^2\Delta_{5/2}}$. This difference can be explained by the dissimilarity in the well depths: D_e = 86 cm^{-1} for $\mathbf{2^2\Sigma_{1/2}}^{+}$ state and 930 cm^{-1} for $\mathbf{1^2\Delta_{5/2}}$ state. The same distinction is also observed for $\mathbf{1^2\Pi_{1/2}}$, $\mathbf{1^2\Pi_{3/2}}$ and $\mathbf{1^2\Delta_{3/2}}$ states.

4. CONCLUSIONS

This study involved an ab initio investigation of nearly 25 electronic states within the $Sr^{+}He$ and SrHe van der Waals systems by combining ab -initio calculation and modeling techniques. We have used the pseudopotential approach and core polarization potentials for the $Sr^{+}He$ ionic system, where an SCF calculation was sufficient to attain potential energy curves for 12 electronic states.

For SrHe neutral system, in addition to the SCF calculations, full valence CI calculations were performed for the two valence electrons interacting with the $Sr^{2+}He$ core−core system. The potential interaction between the Sr^{2+} He cores was obtained from an accurately performed CCSD (T) calculation using the Molpro program.[26] Subsequently, this potential was further refined by fitting it to TT[16] and ELJ[28] analytical potentials to improve its representation at intermediate distances, where the minima of many $Sr^{+}He$ states are situated. The potential energy curves were computed across a broad and densely sampled grid of internuclear distances. The spectroscopic constants of the (1−6) $^2\sum^{+}$, (1−4) $^2\Pi$, (1−2) $^2\Delta$for $Sr^{+}He$, as well as the (1−7) $^{1,3}\Sigma^{+}$, (1−4) $^{1,3}\prod$ and (1−2) $^{1,3}\Delta$electronic states for SrHe, were extracted and compared with existing theoretical works.[7−10,12,14,15]

Excellent agreement is observed between our findings and the theoretical work of Adrian et al. for the ground state of $X^2\Sigma^{+}$. Similarly, for the $2^2\Pi$ excited state, we compared our results with the recent work of Masimo and Cagnomi,[8] revealing consistent agreement in equilibrium distances and well-depths. Notably, this study introduces spectroscopic constants for various higher excited states for the first time. These states exhibit undulations attributed to avoided crossings or undulating orbitals of the atomic Rydberg states.

A comparison of potential energy curves for the $Sr^{2+}He$, $Sr^{+}He$, and SrHe systems reveals the repulsive nature of the electron-helium interaction, particularly evident in $\sum^{+}$ symmetries where orbitals along the molecular axis are involved. In contrast, in Π and Δ symmetries, the repulsive effects are weaker due to the involvement of orbitals perpendicular to the molecular axis.

Moreover, the spin−orbit coupling was incorporated using the semiempirical scheme proposed by Cohen and Schneider.[39] Consequently, this inclusion has resulted in energy splitting and minor shifts in equilibrium distances and transition energies for certain states. The transition dipole moment linking the ground state to the $3^2\Sigma^{+}$ and $2^2\Pi$ excited states, as well as the vibrational energy level spacing $(E_{v+1}-E_v)$ are also influenced by spin−orbit coupling.

The accurate data obtained for the ground state of the ionic $Sr^{2+}He$, $Sr^{+}He$, and neutral SrHe molecular systems will serve as a foundational basis for broader structural and dynamical studies into large $Sr^{2+}He_n$, $Sr^{+}He_n$, and $SrHe_n$ clusters, as well as the embedding of Sr^{2+} and Sr^{+} ions into helium clusters and

https://doi.org/10.1021/acsomega.4c01433
ACS Omega 2024, 9, 32604−32616

Table 7. Vibrational Energy Level Spacing $E_{v+1}-E_v$ of $Sr^{2+}He$ ($X^1\sum^+$) and ($X^2\sum^+$, $1^2\Pi$, $2^2\Pi$, $3^2\Pi$, $4^2\Pi$, $1^2\Delta$ and $2^2\Delta$) of Sr^+He without Spin-orbit Coupling[a]

$Sr^{2+}He$ ($X^1\sum^+$)	$X^2\Sigma^+$	$1^2\Pi$	$2^2\Pi$	$3^2\Pi$	$4^2\Pi$	$1^2\Delta$	$2^2\Delta$
176.972	2.45	172.312	124.035	177.938	162.514	155.762	155.023
150.305		131.414	88.002	129.763	125.451	118.602	118.156
128.490		93.891	57.719	84.791	91.611	86.415	85.95
108.462		62.500	34.371	51.620	62.178	59.979	59.11.
88.074		38.982	18.145	33.590	38.777	39.390	37.857
67.527		22.728	8.271	22.318	22.109	23.889	21.871
48.645		11.741	2.806	12.592	10.946	12.719	10.766
32.886		4.798				5.318	4.059
20.970							
12.505							
6.620							
2.845							
0.913							

[a]All values are in (cm^{-1}).

Table 8. Vibrational Energy Level Spacing $E_{v+1}-E_v$ for Excited States ($3^2\Sigma_{1/}{}^{2+}$, $2^2\Pi_{1/}{}^2$, $2^2\Pi_{3/}{}^2$, $4^2\Pi_{1/}{}^2$, $4^2\Pi_{3/}{}^2$, $2^2\Sigma_{1/}{}^{+2}$, $1^2\Pi_{1/}{}^2$, $1^2\Pi_{3/2}$, $1^2\Delta_{3/2}$ and $1^2\Delta_{5/2}$) of Sr^+He Molecular System with Spin-Orbit Coupling[a]

$3^2\Sigma 1/2^+$ (5p)	$2^2\Pi 1/2$	$2^2\Pi 3/2$	$4^2\Pi 1/2$	$4^2\Pi 3/2$	$2^2\Sigma 1/2^+$	$1^2\Pi 1/2$	$1^2\Pi 3/2$	$1^2\Delta 3/2$	$1^2\Delta 5/2$
4.519	144.010	154.048	182.484	182.172	30.638	176.992	178.87	189.402	176.336
0.347	111.390	129.293	155.962	155.476	19.915	144.565	150.068	160.09	150.04
	12.966	106.296	131.014	130.469	11.041	110.513	122.836	132.994	125.899
	9.431	84.988	107.637	107.079	4.264	73.785	97.125	108.223	103.815
	3.522	65.619	85.894	85.385	0.581	45.962	73.597	85.898	83.627
		48.176		65.680		33.208	53.88	66.084	65.316
		33.037		48.261		23.394	38.475	48.872	48.925
		20.446		33.302		14.749	25.963	34.074	34.504
		10.763		20.937		7.269	15.734	21.739	22.255
		4.046		10.93			7.642	11.934	12.391
								4.915	5.152

[a]All values are in (cm^{-1}).

nanodroplets. Additionally, the findings related to the excited states of the Sr^+He system can be employed to explore the broadening effect of the Sr^+ spectrum resulting from collisions with helium.

AUTHOR INFORMATION

Corresponding Authors

Jamila Dhiflaoui − *Faculty of Science of Monastir, Laboratory of Interfaces and Advanced Materials LR11ES55, Physics Department, University of Monastir, 5019 Monastir, Tunisia;* orcid.org/0000-0002-3827-3499; Email: jamila.dhiflaoui@ipeim.u-monastir.tn

Hamid Berriche − *Faculty of Science of Monastir, Laboratory of Interfaces and Advanced Materials LR11ES55, Physics Department, University of Monastir, 5019 Monastir, Tunisia; Department of Mathematics and Physics School of Arts and Sciences, American University of Ras Al Khaimah, Ras Al Khaimah, United Arab Emirates;* orcid.org/0000-0002-1442-669X; Email: hamid.berriche@aurak.ac.ae

Authors

Mohamed Bejaoui − *Faculty of Science of Monastir, Laboratory of Interfaces and Advanced Materials LR11ES55, Physics Department, University of Monastir, 5019 Monastir, Tunisia*

Wissem Zrafi − *Faculty of Science of Monastir, Laboratory of Interfaces and Advanced Materials LR11ES55, Physics Department, University of Monastir, 5019 Monastir, Tunisia;* orcid.org/0000-0001-9954-7361

Complete contact information is available at: https://pubs.acs.org/10.1021/acsomega.4c01433

Author Contributions

All authors have contributed equally in the preparation of the manuscript.

Funding

The authors have no affiliation with any organization with a direct or indirect financial interest in the subject matter discussed in the paper.

Notes

The authors declare no competing financial interest.

Ethical Approval: This paper does not contain any studies with human participants or animals performed by any of the authors.

ACKNOWLEDGMENTS

The authors thank the anonymous referees for their careful reading of the manuscript and their careful reading of the manuscript and their fruitful comments and suggestions.

REFERENCES

(1) Alford, W. J.; Burnett, K.; Cooper, J. Polarization of collisionally redistributed light from the far wings of strontium-rare-gas systems. *Phys. Rev. A* **1983**, *27*, 1310.

(2) Harima, H.; Yanagisawa, T.; Tachibana, K.; Urano, Y. Absorption coefficients for the wings of the Sr resonance line at 4607 AA broadened by He Ne and Kr. *J. Phys. A: Math. Gen.* **1983**, *16*, 4365.

(3) Ueda, K.; Komatsu, T.; Sato, Y. Observation of collision-induced-dipole absorption bands in strontium−rare-gas mixtures I The 5s−4d bands. *J. Chem. Phys.* **1989**, *91*, 4495.

(4) Chan, Y. C.; Gelbwachs, J. A. Broadening shifting and asymmetry of the strontium resonance line induced by rare gas perturbers. *J. Phys. B* **1992**, *25*, 3601.

(5) Redondo, C.; Sánchez Rayo, M. N.; Ecija, P.; Husain, D.; Castaño, F. Collisional dynamics of low energy states of atomic strontium following the generation of $Sr(5s5p\,^1P_1)$ in the presence of Ne Kr and Xe. *Chem. Phys. Lett.* **2004**, *392*, 116.

(6) Zhu, R. S.; Han, K. L.; Huang, J. H.; Zhan, J. P.; He, G. Z. Theoretical study of the potential energy curves for CaAr and SrAr systems. *Bull. Chem. Soc. Jpn.* **1998**, *71*, 2051.

(7) Stienkemeier, F.; Meier, F.; Stark, K.; Lutz, H. O. Alkaline earth metals (Ca Sr) attached to liquid helium droplets: Inside or out? *J. Chem. Phys.* **1997**, *107*, 10816.

(8) Mella, M.; Cagnoni, F. Exciplexes with Ionic Dopants: Stability Structure and Experimental Relevance of $M^+(^2P)^4He_n$ (M = Sr Ba). *J. Phys. Chem. A* **2014**, *118*, 6473.

(9) Gardner, A. M.; Withers, C. D.; Graneek, J. B.; Wright, T. G.; Viehland, L. A.; Breckenridge, W. H.; et al. Theoretical Study of the Bonding in M^{n+}-RG Complexes and the Transport of M^{n+} Through Rare Gas (M = Ca Sr and Ra; n = 1 and 2; and RG = He−Rn). *J. Chem. Phys.* **2010**, *132*, No. 054302.

(10) Kleinekathöfer, U. Accurate *ab initio* pair potentials between helium and the heavier group 2 elements. *Chem. Phys. Lett.* **2000**, *324*, 403.

(11) Giusti-Suzor, A.; Roueff, E. Depolarization broadening and shift of Sr II and Ca II lines by helium atoms. *J. Phys. B* **1975**, *8*, 2708.

(12) Harima, H.; Ihara, T.; Urano, Y.; Tachibana, K. Potential Calculation for Alkaline-Earth-Metal-Ion−Rare-Gas-Atom Pairs and its Application to Line-Core Analysis. *Phys. Rev. A* **1986**, *34*, 2911.

(13) Baylis, W. E. Semiempirical Pseudopotential Calculation of Alkali−Noble-Gas Interatomic Potentials. *J. Chem. Phys.* **1969**, *51*, 2665.

(14) Lovallo, C. C.; Klobukowski, M. Accurate ab initio pair potentials between helium and the heavier group 2 elements. *J. Chem. Phys.* **2004**, *120*, 246.

(15) Yin, G. P.; Li, P.; Tang, K. T. The ground state Van der Waals potentials of the strontium dimer and strontium rare-gas complexes. *J. Chem. Phys.* **2010**, *132*, No. 074303.

(16) Tang, K. T.; Toennies, J. P. J. An Improved Simple Model for the van der Waals Potential Based on Universal Damping Functions for the Dispersion Coefficients. *Chem. Phys.* **1984**, *80*, 3726.

(17) Kreis, C.; Holdener, M.; Génévriez, M.; Merkt, F. High-resolution photoelectron spectroscopy of the ground and first excited electronic states of $MgKr^+$. *Mol. Phys.* **2023**, *121*, 117−118.

(18) Kreis, C.; Schmitz, J. R.; Merkt, F. High-resolution photoelectron spectroscopy of the very weakly bound MgNe molecule. *Mol. Phys.* **2024**, e2297814.

(19) Bejaoui, M.; Dhiflaoui, J.; Mabrouk, N.; Eloualhazi, R.; Berriche, H. Theoretical Investigation of The Electronic Structure and Spectra of $Mg^{2+}He$ And Mg^+He. *J. Chem. Phys. A* **2016**, *120*, 747.

(20) Dhiflaoui, J.; Berriche, H.; Heaven, M. Theoretical investigation of RbXe and CsXe excimers including the spin−orbit interaction. *J. Phys. B: AI. Mol. Phys.* **2016**, *49*, No. 205101.

(21) Dhiflaoui, J.; Berriche, H. One-Electron Pseudopotential Investigation of CsAr van der Waals System Including the Spin−Orbit Interaction. *J. Phys. Chem. A* **2010**, *114*, 7139.

(22) Dhiflaoui, J.; Berriche, H.; Herbane, M.; Al Sehimi, M. H.; Heaven, M. C. Electronic Structure and Spectra of the RbAr van der Waals System Including Spin−Orbit Interaction. *J. Phys. Chem. A* **2012**, *116*, 10589.

(23) Berriche, H. Electronic Spectra and Spin Orbit Interaction for FrAr van der Waals System. *Int. J. Quantum Chem.* **2013**, *113*, 1349.

(24) Dhiflaoui, J.; Bejaoui, M.; Berriche, H. Electronic structure and spectra of the RbHe van der Waals system including spin orbit interaction. *Eur. Phys. J. D* **2017**, *71*, 331.

(25) Zrafi, W.; Bejaoui, M.; Dhiflaoui, J.; Farjallah, M.; Berriche, H. Non-relativistic and relativistic investigation of the low-lying electronic states of Sr^{2+} Xe Sr^+ Xe and SrXe systems. *Eur. Phys. J. D* **2019**, *73*, 60.

(26) Werner, H. J.; Knowles, P. J.; Knizia, G.; Manby, F. R.; Schütz, M.*MOLPRO Version 2010.1, A Package of Ab-initio Programs*, 2010, http://www.molpro.net.

(27) Alharzali, N.; Berriche, H.; Villarreal, P.; Prosmiti, R. Theoretical Study of Cationic Alkali Dimers Interacting with He: Li_2^+−He and Na_2^+−He van der Waals Complexes. *J. Phys. Chem. A* **2019**, *123*, 7814−7821.

(28) Hay, P. J.; Wadt, W. R. Ab initio effective core potentials for molecular calculations Potentials for K to Au including the outermost core orbitals. *J. Chem. Phys.* **1985**, *82*, 299.

(29) Schwerdtfeger, P.; Gaston, N.; Krawczyk, R. P.; et al. Extension of the Lennard-Jones potential: Theoretical investigations into rare-gas clusters and crystal lattices of He Ne Ar and Kr using many-body interaction expansions. *Phys. Rev. B* **2006**, *73*, No. 064112.

(30) Thomas, M. A.; Humberston, J. W. The polarizability of helium. *J. Phys. B: Atom. Mol. Phys.* **1972**, *5*, L229.

(31) Yang, C. L.; Zhang, X.; Han, K. L. Theoretical study on analytical potential function and spectroscopic parameters for CaF molecule. *J. Mol. Structure: THEOCHEM* **2004**, *678*, 183.

(32) Durand, P.; Barthelat, J. C. Theoretical Method to Determine Atomic Pseudopotentials for Electronic Structure Calculations of Molecules and Solids. *Theor. Chem. Acta.* **1975**, *38*, 283.

(33) Foucrault, M.; Millié, P.; Daudey, J. P. Non perturbative Method for Core−Valence Correlation in Pseudopotential Calculations: Application to The Rb_2 and Cs_2 Molecules. *J. Chem. Phys.* **1992**, *96*, 1257.

(34) Müller, W.; Flesh, J.; Meyer, W. Treatment of Inter Shell Correlation Effects in Abinitio Calculations by Use of Core Polarization Potentials Method and Application to Alkali and Alkaline Earth Atoms. *J. Chem. Phys.* **1984**, *80*, 3297.

(35) Coker, H. Empirical Free-Ion Polarizabilities of the Alkali Metal Alkaline Earth Metal and Halide Ions. *J. Phys. Chem. A* **1976**, *80*, 2078.

(36) NIST ASD Team. *NIST Atomic Spectra*, The National Institute of Standards and Technology http://physics.nist.gov.

(37) Belayouni, S.; Ghanmi, C.; Berriche, H. Adiabatic and quasi-diabatic investigation of the strontium hydride cation SrH^+: structure spectroscopy and dipole moments. *Can. J. Phys.* **2016**, *94* (9), 791−802.

(38) *CRC Handbook of Chemistry and Physics*, 76th ed.; Lide, D. R., Ed.; CRC: Boca Raton, 1995.

(39) Cohen, J. S.; Schneider, B. Ground and Excited States of Ne_2 and Ne^{2+}: Potential Curves With and Without Spin-Orbit Coupling. *J. Chem. Phys.* **1974**, *61*, 3230.

(40) Berriche, H.; Gadea, F. X. Ab initio study of the LiH^+ molecule electronic interaction analysis and LiH UV photoelectron spectrum. *Chem. Phys.* **1995**, *191*, 119−131.

(41) Akkari, S.; Zrafi, W.; Ladjimi, H.; Bejaoui, M.; Dhiflaoui, J.; Berriche, H. Electronic structure of ground and low-lying excited states of $BaLi^+$ molecular ion: spin-orbit effect radiative lifetimes and Franck-Condon factor. *Phys. Scr.* **2024**, *99*, No. 035403.

(42) Ladjimi, H.; Zrafi, W.; Farjallah, M.; Bejaoui, M.; Berriche, H. Electronic structure cold ion−atom elastic collision properties and possibility of laser cooling of BeCs+ molecular ion. *Phys. Chem. Chem. Phys.* **2022**, *24*, 18511−18522.

(43) Zrafi, W.; Ladjimi, H.; Said, H.; Berriche, H.; Tomza, M. Ab initio electronic structure and prospects for the formation of ultracold

https://doi.org/10.1021/acsomega.4c01433
ACS Omega 2024, 9, 32604−32616

calcium−alkali-metal-atom molecular ions. *New J. Phys.* **2020**, *22*, No. 073015.
(44) Zrafi, W.; Ladjimi, H.; Berriche, H. Accurate ab initio calculations of adiabatic energy and dipole moment: Prospects for the formation of cold Alkaline-Earth-Francium molecular ions ALKE-Fr^+ (ALKE = Be Mg Ca and Sr). *Phys. Scr.* **2023**, *98*, No. 125403.

https://doi.org/10.1021/acsomega.4c01433
ACS Omega 2024, 9, 32604−32616